Author Manuscript

Author Manuscript

Author Manuscript

Author Manuscript

HHS Public Access

Author manuscript

Xenotransplantation. Author manuscript; available in PMC 2017 May 26.

Published in final edited form as:

Xenotransplantation. 2016 May ; 23(3): 211–221. doi:10.1111/xen.12235.

Magneto-encapsulated human islets xenotransplanted into swine: A comparison of different transplantation sites

D.R. Arifin[1,2,#,*], **S. Valdeig**[3,#], **R.A. Anders**[4], **J.W.M. Bulte**[1,2,5,6,7], and **C.R. Weiss**[3]

[1]Division of MR Research, Russell H. Morgan Dept. of Radiology and Radiological Science, The Johns Hopkins University School of Medicine, Baltimore, MD 21205, USA

[2]Institute for Cell Engineering, Cellular Imaging Section and Vascular Biology Program, The Johns Hopkins University School of Medicine, Baltimore, MD 21205, USA

[3]Interventional Radiology Center, Russell H. Morgan Dept. of Radiology and Radiological Science, The Johns Hopkins University School of Medicine, Baltimore, MD 21205, USA

[4]Gastrointestinal Liver Pathology, Dept. of Pathology, The Johns Hopkins University School of Medicine, Baltimore, MD 21205, USA

[5]Dept. of Chemical & Biomolecular Engineering, The Johns Hopkins University School of Medicine, Baltimore, MD 21205, USA

[6]Dept. of Biomedical Engineering, The Johns Hopkins University School of Medicine, Baltimore, MD 21205, USA

[7]Dept. of Oncology, The Johns Hopkins University School of Medicine, Baltimore, MD 21205, USA

Abstract

Background—The fate of magnetically-labeled, barium-gelled Alginate/Protamine Sulfate/Alginate microcapsules (APSA magnetocapsules) following xenotransplantation was assessed by magnetic resonance imaging (MRI) and histopathology.

Methods—Magnetocapsules with and without human islets were transplanted into 5 different clinically accessible sites of swine: portal vein, subcutaneous tissue, skeletal muscle, the liver and kidney subcapsular space. The surface of APSA magnetocapsules was modified using clinical grade heparin to mitigate an instant blood-mediated inflammatory reaction.

Results—The accuracy of site-specific delivery was confirmed using a clinical 1.5T MRI setup, where the magnetocapsules appeared as distinct hypointense entities upon transplantation. As proven by the Lee While blood coagulation test, heparin-treated APSA magnetocapsules did not

[*]Corresponding author: Dian Arifin, Ph.D., Department of Radiology and Radiological Science, Institute for Cell Engineering, The Johns Hopkins University School of Medicine, Address: Miller Research Building, suite 652, 733 N. Broadway, Baltimore, MD 21205, dianrarifin@yahoo.com, phone: 443-683-5679.

[#]Shared first authorship

Author contributions

Concept/design: J.W.M.B, C.R.W., D.R.A.; Data analysis/interpretation: D.R.A., S.V., R.A.A., J.W.M.B, C.R.W.; Drafting article: D.R.A.; Preparation of tables and figures: D.R.A., S.V.; Critical revision of article: J.W.M.B., C.R.W.; Approval of article: S.V., R.A.A., J.W.M.B., C.R.W.; Data collection: D.R.A., S.V., R.A.A., C.R.W.; Funding secured by: J.W.M.B.; C.R.W.

Author Manuscript Author Manuscript Author Manuscript Author Manuscript

induce blood clotting for more than 48 hours *in vitro*. However, heparinized magnetocapsules induced innate and adaptive immune responses *in vivo* regardless of the transplantation site.

Conclusions—We have demonstrated the feasibility of using a clinical 1.5T magnetic resonance imaging to non-invasively detect the accuracy of APSA magnetocapsule injection into various clinically accessible transplantation sites. Among the investigated transplantation sites, the liver and kidney subcapsular space were found to be the least immune-responsive towards xenografted encapsulated islets.

Keywords

Diabetes; islet; large animal model; MRI; microcapsule

Introduction

Insulin independence in type I diabetes (TD1M) patients can potentially be achieved by pancreatic islet cell therapy. The development of the Edmonton protocol [1–3] for islet isolation from cadaveric donors followed by allotransplantation into the portal vein has been seen as a major improvement in this form of treatment. This protocol, however, requires life-long immunosuppressive therapy which is associated with serious side effects and significant medical costs. Moreover, the severe shortage of donor human islets may necessitate the use of islets extracted from non-human sources. The recent success of porcine islet xenotransplantation to reverse diabetes in non-human primates [4–6] has raised hope to use this approach to treat TD1M patients [7].

A means for long-term prevention of transplant rejection without the use of potentially toxic immunosuppressive drugs is critical for the success of islet cell therapy. One such possible means is microencapsulation where islets are isolated from the host immune system by enclosure inside semi-permeable microcapsules composed of alginate [8–10]. Alginate hydrogel is a preferred material for islet encapsulation due to its biocompatibility, availability and relative ease of microcapsule formation [11]. Numerous alginate-based microcapsule systems have been developed with varying success rates [8, 11–13] . A promising microcapsule design is barium or calcium-gelled alginate microcapsules which are prepared from purified alginate and coated with a double-layered polyelectrolyte complex [11, 12, 14]. The coating is necessary to regulate the permeability of the capsules, to strengthen the capsule walls, and to cover potentially protruding cells. Poly-L-lysine (PLL) is conventionally used as a polycationic cross-linker to ionically bind the outer alginate layer to alginate capsules [14–16]. However, the interest in PLL diminished as strong inflammatory responses were observed in some cases [17], possibly due to inadequate PLL binding. A newly developed multilayered capsule design using PLL may resolve this biocompatibility issue [18].

A more recent candidate for a polycationic cross-linker is poly-L-ornithine (PLO). Indeed, the commercialization and clinical trials of Ca^{2+-} gelled alginate/PLO/alginate encapsulated islets are in progress. Living Cell Technologies (Manukau, New Zealand) adapted this microcapsule design for commercialization of encapsulated porcine islets under the tradename Diabecell. The first report of phase I/IIa clinical trials in New Zealand showed

Author Manuscript Author Manuscript Author Manuscript Author Manuscript

that encapsulated porcine islets reduced the numbers of unaware hypoglycemia events and the daily total insulin dose at one year after transplantation without the use of immunosuppressive drugs in the majority of the patients [19].

In order to develop alginate microcapsules cross-linked with clinical-grade polycationic polymer, we introduced a novel formulation called barium-gelled alginate/protamine sulfate/alginate (APSA) microcapsules as reported in our previous publication [20]. We created a double-layered alginate microcapsules using Ba^{2+} as a gelating cation and the protamine residues from clinical-grade protamine sulfate (PS) as a new polycationic cross-linker. PS is an FDA-approved drug that reverses the activity of heparin. We measured that less than 1 nM of barium ions were actually bound to the alginate, which was much lower than the cytotoxic level of free barium ions (5–10 mM). APSA microcapsules possessed a diameter of 444±21 μm (coefficient of variation=0.05), were mechanically stronger, and supported higher cell viability compared to conventional alginate/PLL/alginate capsules (APLLA). Double-layered capsules were typically impermeable to molecules larger 120 kDa [21] to prevent the invasion of immunoglobulins. Our past work with APSA capsules demonstrated successful immunoprotection and therapeutic efficacy of implanted encapsulated beta cells in hyperglycemic mouse models without the use of immunosuppressive drugs [22].

To enable MRI-visibility, microcapsules were labeled with superparamagnetic iron oxide nanoparticles. Our previous study [21] showed that the viability and bio-function (as measured by human c-peptide secretion) of human islets inside magnetically labeled microcapsules (magnetocapsules) were not statistically different than those inside unlabeled capsules for at least two weeks *in vitro*. This indicated that the magnetic labeling of the microcapsules had no adverse effects on islet viability and bio-function. We also demonstrated that magnetocapsules transplanted in the liver of swine via portal vein injection could be imaged by a clinical MRI.

Due to the high perfusion and vascular density of the liver, portal vein is considered to be one of the ideal transplantation sites for unencapsulated islets [2, 3]. The disadvantages of portal vein transplant of encapsulated islets include possible obstruction of the microcapillary liver network by microcapsules. In addition, microcapsule transplants in the portal vein could not be retrieved for testing, viability assessment and in case of therapy failure. In this study therefore, APSA magnetocapsules were transplanted into alternative clinically accessible transplantation sites, namely the subcutaneous tissue, skeletal muscle, the kidney subcapsular and liver subcapsular space. The liver portal vein site was included for comparison.

In clinical applications, the delivery of microcapsules into each transplantation site tested in this study can easily be performed under ultrasound and fluoroscopic (portal vein access) guidance. However, ultrasound has a limited depth of penetration, limited field of view and, overall, a lower resolution when compared to CT and MRI. This makes imaging sub-millimeter structures, such as microcapsules, using ultrasound difficult if not impossible. Furthermore, despite the fact that x-ray-visible microcapsules have been developed [22–25], there are concerns surrounding side effects of repeated exposure to X-ray radiation during CT imaging sessions, particularly in children and women of childbearing age. On the other

Author Manuscript Author Manuscript Author Manuscript Author Manuscript

hand, MRI is able to provide high resolution imaging, with excellent soft tissue and anatomic detail over a large field of view without exposure to ionizing radiation. MRI is also useful for percutaneous biopsy since it allows for highly targeted sampling and evaluation of transplants over time [26]. Because of this, we used MRI to image magnetocapsules and their target organs in this study.

In light of a recent interest and development in xenotransplantation of non-human islets into human patients [7], we elected to transplant encapsulated human islets into swine in order to simulate a xenotransplantation paradigm. We decided to use human islets because there is no consensus yet on which non-human islets are the best for treatment of human diabetic patients. Moreover, the “replacements” of human islets should have the characteristics of human islets regardless of their origins. The swine model is a clinically relevant choice because of its similarity to human anatomy and physiology. The size and anatomy of swine organs and transplantation sites resemble those of an adult human. As well, humans and swine have similar immune system-related genes, proteins and immune responses, and therefore swine has been deemed a suitable model for xenotransplantation studies in clinical translations [27]. Rodent models on the other hand have smaller organs and demonstrate different immune responses compared to human. Therefore, investigating the feasibility of MRI techniques, microcapsule biocompatibility and potential transplantation sites for clinical translations necessitated the use of a swine model.

The aims of this study were: 1) to evaluate the feasibility of using clinical MRI to non-invasively detect the accuracy of APSA magnetocapsule injection into various clinically accessible transplantation sites other than portal vein, and 2) to assess the host immune and foreign body responses in each transplantation site, in order to find the least immune-responsive area towards xenotransplanted APSA magnetoencapsulated islets.

Materials and Methods

1. Human pancreatic islets

Cadaveric human pancreatic islets were purchased through the Integrated Islet Distribution Program (City of Hope, CA). Human islets with a minimum viability and purity of 80%/80% were used throughout the experiments. Islets were encapsulated one day after extraction from the donor, and cultured for one day prior to transplantation in CMRL1066 medium (Mediatech, Manassas, VA), supplemented with 10% fetal bovine serum (Gemini Bio-Products, West Sacramento, CA), and 1% penicillin/streptomycin (Sigma-Aldrich, St. Louis, MO).

2. Microcapsule preparation

2.1. Synthesis of alginate microcapsules—Pronova ultrapure alginates were purchased from Nova Matrix (Sandvika, Norway). Low viscosity guluronate (LVG) alginate is a low-viscosity (20–200 mPas) sodium alginate where 60% of the monomers are guluronate, while low viscosity mannuronate (LVM) alginate has 50% mannuronate monomers. Chromogenic endotoxin tests of alginate solutions and microcapsule suspensions revealed endotoxin levels in the liquid samples to be below the detection limit of the assay

Author Manuscript Author Manuscript Author Manuscript Author Manuscript

(0.005 EU/ml or ~0.25 EU/g). The endotoxin tests were repeated five times. Human pancreatic islets (16,000–17,000 islets per ml of alginate to obtain approximately 1–2 islets per capsule) were suspended in 2% w/v LVG alginate. Alginate microcapsules were formed using an electrostatic droplet generator, and were immediately gelated in a 20 mM $BaCl_2$ solution. The capsules were washed twice with 0.9% w/v NaCl + 10 mM HEPES, and subsequently cross-linked for 5 minutes with 0.05% w/v protamine sulfate (APP Pharmaceuticals, Schaumburg, IL) to form alginate/protamine sulfate/alginate (APSA) capsules or poly-L-lysine hydrobromide (Mw=15–30 kDa, Sigma-Aldrich, St. Louis, MO) to form alginate/poly-L-lysine/alginate (APLLA) capsules. After a second saline washing, the outer surface of the capsules was cross-linked with 0.15% w/v LVM alginate for 5 minutes, followed by a final saline washing. All solutions were prepared in 0.9% w/v NaCl + 10 mM HEPES. In order to create theranostic, MRI-visible and immunoprotective APSAH magnetocapsules [21, 23, 28–30], 10% v/v Feridex® (AMAG Pharmaceuticals, Waltham, MA) was mixed with LVG alginate prior to microcapsule formation to give a final LVG alginate concentration of 2% w/v.

2.2. Microcapsule coating with heparin—Either APSA or APLLA capsules were mixed with 500 units/ml of clinical grade heparin for 5 minutes on a horizontal rocker. Heparin solution was prepared in 0.9% w/v NaCl + 10 mM HEPES.

3. *In vitro* studies

3.1. Blood coagulation test—A Lee-White blood coagulation test [31] was performed using blood from two healthy adult domestic female swine (35–45 kg) for evaluating heparin-treated APLLA and APSA microcapsules. Heparin-treated empty microcapsules were washed five times with 0.9% saline+10 mM HEPES after a heparin treatment to remove unbound heparin. One ml of freshly collected blood was mixed with one ml of capsule suspension (~3000 capsules) in a glass test tube, and immersed in a 37°C degree water bath. The controls were one ml of blood mixed with one ml of 0.9% saline+10 mM HEPES without capsules, and one ml of blood mixed with empty APLLA or APSA microcapsules without a heparin treatment. The mixture was lightly agitated and observed every 20 seconds. The time when blood clotted was then recorded. The experiment was repeated six times.

4. *In vivo* studies

4.1. Animals—This study was approved by our Institutional Animal Care and Use Committee. Eight healthy female domestic swine (35–45kg) were used for transplantation of heparin-treated APSA (APSAH) magnetocapsules according to Table 1. Blood samples were taken before and every day after transplantation. Blood plasma was collected by centrifuging blood samples at 1000xg for 20 minutes at 4°C. For all swine, CBC and blood chemistry panels were obtained prior to microcapsule transplantation, and once every week thereafter, and on the day of sacrifice.

4.2. Magnetocapsule transplantation and imaging protocol—All transplantations were performed under sterile conditions and general anesthesia. Swine were fasted 12 hours prior to transplantation. Initial anesthesia was induced by an intramuscular injection of TKX

Author Manuscript Author Manuscript Author Manuscript Author Manuscript

(100 mg/ml telazol, 100 mg/ml ketamine and 100 mg/ml xylazine) at a dose of 1 ml per 22.8 kg body weight. An intravenous catheter was placed in the swine's ear vein for the administration of 0.9% saline throughout the surgical procedure. The swine were intubated and mechanically ventilated with 1–2% isoflurane for maintenance of general anesthesia.

Encapsulation of human islets, transplantation sites and survival end points are given in Table 1. The portal vein was accessed using a direct percutaneous access technique. After a small stab incision, and a 22G Chiba needle was used to access the portal system from the right lateral approach under fluoroscopic and ultrasound guidance. Contrast (Oxilan 350, Guerbet LLC, Bloomington, IN) injection was performed to confirm needle location on X-ray fluoroscopy (Allura Xper FD20, Philips, Andover, MA). A 0.018"Nitrex Guidewire (ev3 Endovascular, Inc., Plymouth, MN) was then advanced into the portal vein. Over this wire, a 4.0Fr ID Neff set (inner diameter ~1.2 mm, Cook Inc., Bloomington, IN) was advanced into the portal system and was used to inject microcapsules. Baseline portal venous pressure and portal venograms were obtained. $1.4–1.5\times10^5$ magnetocapsules were suspended in about 400 ml of sterile heparinized saline, gently agitated to prevent settling, and then slowly infused into the portal vein through the sheath. Immediately after capsule injection, portal venous pressure and portal venograms were again obtained. The needle track was then embolized with a gelfoam slurry (Pfizer, New York, NY). The delivery of magnetocapsules into the liver subcapsular and kidney subcapsular space, skeletal muscle and subcutaneous tissue of the hind limb ($3.3–3.5\times10^4$ magnetocapsules per site, 5 ml) was performed percutaneously using an 18 G trochared needle (inner diameter = 0.84 mm, Cook Inc., Bloomington, IN) under ultrasound guidance (Sonosite 180 Plus, SonoSite Inc., Bothell, WA, USA). One needle access was needed for delivery. Delivered magnetocapsules spread in the transplantation sites at the time of injection. To assess the *in vivo* transplantation of injected magnetocapsules in the liver subcapsular and kidney subcapsular space, multi-planar fat saturated T1-weighted high resolution flash 3D-Volume Interpolated Breathhold Examination (VIBE) pre- and post-contrast gadopentetate dimeglumine (Gd-DTPA) (Magnevist, Bayer HealthCare LLC, Wayne, NJ) MR scans were acquired immediately after magnetocapsule injection. Gd-DTPA was injected at a dose of 0.2 mmol Gd/kg body weight for providing contrast for transplantation site. Images were obtained using an 1.5T MR Scanner (MAGNETOM Espree, Siemens Healthcare, Erlangen, Germany) using body and spine matrix coils, and the following parameters: repetition time (TR)=5.0–5.4ms; echo time (TE)=1.8–2.3ms; matrix size=192–256×224–256, field of view (FOV)=23.4–32.0×24.3–32.0 cm, bandwidth 300–355 Hz/Px, and Generalized Autocalibrating Partial Parallel Acquisition (GRAPPA) acceleration factor of 2. Empty magnetocapsules were transplanted into the liver subcapsular space and kidney subcapsular space of three swine. Magnetoencapsulated islets were transplanted into kidney subcapsular space of two swine, while other transplantation variables were applied to one swine per experiment.

5. Histopathological analysis

Tissues were extracted immediately after euthanasia by a lethal injection of sodium pentobarbital. Tissues were fixed in 4% formalin, embedded in paraffin, cut in 5 μm sections, and stained with hematoxylin and eosin H&E) for histopathological analysis. Microscopic images were taken at 10x magnification. Five tissue slides per swine per

Author Manuscript Author Manuscript Author Manuscript Author Manuscript

transplantation site were coded and randomized for blinded histopathological examination. A histopathological scoring scale from 0–3 was created, with 0 = no fibrosis and 3 = greatest degree of fibrosis (Figure 1). To examine the host immune response in greater detail, we divided the overall histopathology score (OHS) into an innate immune response (IIR) versus a foreign body response (FBR). In addition, we differentiated between inflammatory immune responses versus fibrotic stromal immune response (Table 1).

An assessment of the occurrence of an innate IIR was made based on the absence or presence of eosinophils and neutrophils. For the assessment of FBR, the absence or presence of granuloma was determined. Both the inflammatory immune response and the stromal immune response were assessed based on the absence/presence of an inflammatory and stromal fibrosis. For all immune response types, we calculated the average values of the five tissue slides per swine per transplantation site with the absence as 0 and the presence as 1 (Table 1).

We then analyzed the circumferential immune response of a capsule slice with a minimum diameter of 150 μm quantitatively at 10x magnification. The distance from the microcapsule outer edge along 2–4 orthogonal lines to the maximum boundary of surrounding immune cells was measured. For accurate measurements, tissue samples with single microcapsules were selected instead of clusters of multiple capsules. The results were expressed as thickness of immune responses (TIR).

Results

The effect of microcapsule formulation on blood clotting

APSA or APLLA microcapsules contained one human islet equivalent per capsule on average as shown in Figure 2A. Due to the presence of Feridex®, the magnetocapsules exhibited a typical colored appearance (Figure 2B). Before initiating *in vivo* transplantation studies, our first objective was to minimize instant blood-mediated inflammatory response (IBMIR) by modifying the surface of the microcapsules using heparin, which is a clinical anti-blood coagulant agent. The various microcapsule formulations that were tested for their blood clotting properties *in vitro* are listed in Table 2. We found that coating the capsule surface (both unlabeled and magnetically labeled capsules) with heparin dramatically prolonged the *in vitro* clotting time to more than 48 hours after mixing the treated capsules with swine blood (Figure 3), while the controls (blood mixed with non-treated microcapsules or saline+HEPES) coagulated in less than 5 minutes. Considering the results from the blood coagulation test, and a previous study that showed that APSA capsules were stronger and supported higher cell viability compared to conventional APLLA capsules [20], we selected heparin-treated APSA (APSAH) microcapsules as our most promising capsule formulation for further swine studies.

Imaging of transplanted magnetocapsules in swine models

We demonstrated that a clinical 1.5T MRI scanner could be used to non-invasively visualize and confirm the delivery of magnetocapsules in various clinically relevant transplantation sites, where magnetocapsules appeared as hypointense signal entities (Fig. 4). CBC and

Author Manuscript Author Manuscript Author Manuscript Author Manuscript

chemistry panels of all swine were stable before and after transplantation and during the survival period.

Histopathological studies of intraportal vein transplants

The first phase of the study was to inject empty (without islets) APSAH magnetocapsules into the liver portal vein of a healthy swine (swine 1) followed by animal sacrifice at one hour after capsule transplantation. We observed no to weak immune cell infiltration or circumferential responses as indicated by the histology and TIR scores in Table 1. Circumferential response was manifested in the form of fibrotic tissue surrounding the capsules. An IIR score is based on a combination of eosinophil and neutrophil infiltration, while an FBR score involves giant cells and granuloma.

The portal vein injection experiment was then repeated with empty magnetocapsules (swine 2) and magnetoencapsulated human islets (swine 3). Instead of an immediate sacrifice, the swine were sacrificed two weeks after capsule delivery (Table 1). Circumferential immune reactions were found in both animals at the end of the two-week period, with little difference in the IIR and FBR scores between the two swine. No inflammation was observed with empty capsules but a positive stromal score was present. Inflammation and stromal scores with encapsulated islets were almost the same. Magnetoencapsulated islets induced a stronger circumferential immune response compared to empty magnetocapsules, which was reflected in higher TIR values. The corresponding histopathology of portal vein samples taken from swine 2 and 3 are shown in Figure 5. During the longer survival period, an immune response developed over time as evidenced by higher histology scores and TIR values in swine 1 (survival period of one hour) compared to swine 2 (survival period of two weeks). Immune responses triggered by magnetoencapsulated human islets (swine 3) were stronger than responses towards empty magnetocapsules (swine 2) as xenotransplantation effects induced by human islet transplants further exacerbated the responses.

Histopathological comparison studies of different transplantation sites

Empty APSAH magnetocapsules were transplanted into various sites of a healthy swine (swine 4), specifically the subcutaneous tissue and skeletal muscle of the hind limb, the liver subcapsular space and the kidney subcapsular space. The animal was sacrificed after two weeks. The capsules delivered subcutaneously induced the strongest IIR and FBR, while no IIR and FBR could be detected in the liver subcapsular space or kidney subcapsular space. Inflammation but no stromal responses were observed in the subcutaneous and skeletal muscle, while the opposite was found in the liver subcapsular space and kidney subcapsular space. TIR of skeletal muscle and subcutaneous site were 2–3 times higher compared to liver subcapsular space and kidney subcapsular space. The representative macrophotographs and H&E images are shown in Figure 5 and 6. Among the various transplantation sites tested in this study, the liver subcapsular space and kidney subcapsular space were the least immune-responsive towards transplanted magnetocapsules.

To ensure the results for the liver subcapsular space and kidney subcapsular space (which appeared to be the least immune-responsive sites based on the histology scores and TIR values of swine 4) were reproducible, the experiment was repeated with two more healthy

Author Manuscript Author Manuscript Author Manuscript Author Manuscript

animals (swine 5 and 6). A slight increase in IIR was found in the liver subcapsular space, while the other scores remain the same as in the prior experiment.

We proceeded to further study the fate of human islet xenotransplanted in the liver subcapsular space and kidney subcapsular space compared to liver portal vein transplants. Magnetoencapsulated human islets were injected into the liver subcapsular space and kidney subcapsular space in healthy swine (swine 7 and 8). In both transplantation sites, magnetoencapsulated islets induced stronger IIR, FBR and IS than empty magnetocapsules (swine 4, 5 and 6). Compared to the portal vein injection of magnetoencapsulated islets (swine 3), the kidney and liver subcapsular space showed a reduction in FBR and SS with no effect or an increase in the other scores. The TIR for the liver subcapsular space, however, was almost half than the TIR value for portal vein. The IIR and TIR scores of the liver subcapsular space were less than the kidney subcapsular space. Although immune responses were still observed, the liver subcapsular space and kidney subcapsular space appeared to be less immune-responsive towards magnetoencapsulated islet xenotransplants than that was observed for the liver portal vein.

Discussion

We successfully demonstrated a proof-of-concept that a clinical 1.5T MRI could be used to non-invasively detect transplanted alginate magnetocapsules in clinically relevant transplantation sites. With some transplantation sites (i.e. portal vein), it is easy to confirm accurate, on-target delivery of alginate magnetocapsules at the time of delivery. With other sites (i.e. the liver and kidney subcapsular space), it is difficult to confirm accurate delivery when targeting using ultrasound-guidance. In these locations, MRI is very helpful to demonstrate on-target delivery and magnetocapsule distribution, despite the known limitations of MRI such as artifacts from gas, metal, and motion. To our knowledge, transplantation of magnetoencapsulated islets to clinically relevant transplantation sites in swine models with subsequent confirmation using a clinical MRI system has not been performed prior to this study. MRI proved to be a clinically relevant, non-invasive method for imaging the distribution of magnetocapsules in various transplantation sites after surgery. Another advantage of MRI is that pulse sequences can be designed to quantify magnetocapsule volume and the content of iron labels, as demonstrated in a previous study [30]. MRI can provide visual evidence of the correct delivery as well as quantification of delivered magnetocapsules, which can be presented to patients as an evidence of correct transplantation.

Several groups have reported that when transplanted naked human islets were exposed to blood, an instant blood-mediated inflammatory response (IBMIR) consisting of rapid activation of coagulation and complement system can occur. IBMIR is manifested histologically as islets surrounded by blood clots [32, 33]. We performed Lee White blood coagulation test to evaluate whether heparin, which was bound to microcapsules, retained its effectiveness to attenuate blood clotting. The blood coagulation data demonstrated that heparin-treated APSA capsules (APSAH), either unlabeled or magnetically labeled, did not induce blood coagulation for more than 48 hours *in vitro*, making this a potential solution to the IBMIR problem. The results from the swine study however were much less encouraging.

Author Manuscript Author Manuscript Author Manuscript Author Manuscript

APSAH magnetocapsules transplanted into the portal vein, and therefore were exposed to blood, caused significant immune responses and these responses were intensified when human islets were encapsulated.

We then took a different approach to circumvent the host rejection by searching for the most immune-tolerant transplantation sites. The eyes, testis and brain, where blood-tissue barriers exist, were reported to be tolerant towards transplanted unencapsulated cells [34, 35]. However, these transplantation sites are not clinically suitable for encapsulated cells as they are difficult to access and highly sensitive to organ damage. We therefore explored alternate sites for transplantation of encapsulated islets.

Accessing subcutaneous and intramuscular transplantation sites is much easier than that of the other sites. In case of therapeutic failure, the capsules can be easily retrieved with minimal surgical and anesthetic procedures. While the existence of relative hypovascularity and hypoxia in these two sites could be significant drawbacks, applying vascularization strategies with subcutaneous [36–38] or intramuscular [39, 40] islet transplantation had resulted in successful reversal of hyperglycemia in diabetic rodents. For example, subcutaneous porcine islet xenotransplants embedded in a monolayer cellular device normalized the blood glucose of diabetic primates up to 6 months without immunosuppression [41]. In other recent work [42], autologous naked islet transplantation into the skeletal muscle of healthy swine demonstrated that islet transplants remained alive and functional up to 6 months, with evidence of intra-islet vascularization.

On the other hand, the kidney subcapsular space has a high local oxygen tension and is well-vascularized. It has been repeatedly used for transplantation of naked islets in diabetic rodent [43–45], primate [46] and swine models [47–51], with successful restoration of normoglycemia using either syngeneic, allogeneic, or xenogeneic islets. In diabetic rodents, 200 syngeneic islets transplanted in the kidney subcapsular space yielded normoglycemia, in contrast to 800 islets for portal vein transplantation[45]. In a large animal study, encapsulated porcine islets xenotransplanted into the kidney subcapsular space of healthy primates survived and remained functional for up to 6 months without immunosuppression [52]. We also selected the liver subcapsular space in order to take advantage of the dense vascular network while avoiding direct exposure of transplants to blood that can trigger an IBMIR. To the best of our knowledge, this site has never been tested for islet therapy in small or large animal models. Both kidney and liver subcapsular space are relatively accessible for transplantation and retrieval of encapsulated islets.

Our histopathological analysis revealed that host immune responses were found in all transplantation sites. The immune responses intensified when human islets were encapsulated, compared to empty capsules, due to xenogeneic rejection. However, we observed that the liver subcapsular space and kidney subcapsular space showed the least immune-responsiveness towards transplanted magnetocapsules. Hence, using microcapsule formulations with improved biocompatibility, the subcapsular space of the liver or kidney may prove to be the optimal sites to accommodate and support the use of magnetoencapsulated islets in clinical therapies.

Author Manuscript Author Manuscript Author Manuscript Author Manuscript

Conclusions

We successfully presented proof-of-concept that a clinical 1.5T MRI scanner can be used to non-invasively visualize and confirm the delivery of magnetocapsules into clinically relevant transplantation sites, namely subcutaneous tissue, intramuscular tissue, liver subcapsular space and kidney subcapsular space. Despite encouraging results from our past small animal studies, we observed a robust host responses regardless of the capsule formulation and transplantation site. While future work should be geared towards developing different encapsulation materials and/or surface coatings that have better biocompatibility profiles, we found that the liver subcapsular space and kidney subcapsular space are the least immune-responsive towards transplanted encapsulated islets.

Acknowledgments

This study was funded by The National Institutes of Health (RO1 EB007825, R01 DK106972, J.W.M.B.), The Maryland Stem Cell Research Foundation (MSCRII-0161, J.W.M.B.), a grant from Siemens Healthcare AG (J.W.M.B.) and E. Ring Career Development Award from The Society of Interventional Radiology (C.R.W.).

Abbreviations

APSA	Alginate/protamine sulfate/alginate
APLLA	Alginate/poly-L-lysine/alginate
TD1M	type I diabetes mellitus
PLL	Poly-L-lysine
PLO	Poly-L-ornithine
PS	Protamine sulfate
LVG	Low viscosity guluronate
LVM	Low viscosity mannuronate
APSAH	Heparin-treated alginate/protamine sulfate/alginate
OHS	Overall histopathology score
IIR	Innate immune response
FBR	Foreign body response
IS	Inflammation score
SS	Stromal score
TIR	Thickness of immune responses
IBMIR	Instant blood-mediated inflammatory response
TX	Transplantation site

Author Manuscript Author Manuscript Author Manuscript Author Manuscript

PV	Portal vein
SC	Subcutaneous
SM	Skeletal muscle
LS	Liver subcapsular space
KS	Kidney subcapsular space
Surv	survival period in weeks

References

1. Shapiro J, Lakey J, Paty B, et al. Clinical-islet transplantation in Edmonton - 3-year outcomes and new developments. Diabetes. 2003; 52:A66–A66.
2. Shapiro AM, Ricordi C, Hering BJ, et al. International trial of the Edmonton protocol for islet transplantation. The New England journal of medicine. 2006; 355(13):1318–1330. [PubMed: 17005949]
3. Shapiro AM, Lakey JR, Ryan EA, et al. Islet transplantation in seven patients with type 1 diabetes mellitus using a glucocorticoid-free immunosuppressive regimen. The New England journal of medicine. 2000; 343(4):230–238. [PubMed: 10911004]
4. Hering BJ, Wijkstrom M, Graham ML, et al. Prolonged diabetes reversal after portal xenotransplantation of wild-type porcine islets in immunosuppressed nonhuman primates. Nat Med. 2006; 12(3):301–303. [PubMed: 16491083]
5. Hecht G, Eventov-Friedman S, Rosen C, et al. Embryonic pig pancreatic tissue for the treatment of diabetes in a nonhuman primate model. Proc Natl Acad Sci U S A. 2009; 106(21):8659–8664. [PubMed: 19433788]
6. van der Windt DJ, Bottino R, Casu A, et al. Long-term controlled normoglycemia in diabetic non-human primates after transplantation with hCD46 transgenic porcine islets. Am J Transplant. 2009; 9(12):2716–2726. [PubMed: 19845582]
7. Hering BJ, Cooper DK, Cozzi E, et al. The International Xenotransplantation Association consensus statement on conditions for undertaking clinical trials of porcine islet products in type 1 diabetes--executive summary. Xenotransplantation. 2009; 16(4):196–202. [PubMed: 19799759]
8. Dolgin E. Encapsulate this. Nat Med. 2014; 20(1):9–11. [PubMed: 24398953]
9. de Vos P, Lazarjani HA, Poncelet D, Faas MM. Polymers in cell encapsulation from an enveloped cell perspective. Adv Drug Deliv Rev. 2014; 67–68:15–34.
10. Opara EC, Kendall WF Jr. Immunoisolation techniques for islet cell transplantation. Expert Opin Biol Ther. 2002; 2(5):503–511. [PubMed: 12079486]
11. Paredes Juarez GA, Spasojevic M, Faas MM, de Vos P. Immunological and technical considerations in application of alginate-based microencapsulation systems. Front Bioeng Biotechnol. 2014; 2:26. [PubMed: 25147785]
12. Calafiore R, Basta G. Clinical application of microencapsulated islets: actual prospectives on progress and challenges. Adv Drug Deliv Rev. 2014; 67–68:84–92.
13. Orive G, Emerich D, De Vos P. Encapsulate this: the do's and don'ts. Nat Med. 2014; 20(3):233. [PubMed: 24603789]
14. Ponce S, Orive G, Hernandez R, et al. Chemistry and the biological response against immunoisolating alginate-polycation capsules of different composition. Biomaterials. 2006; 27(28):4831–4839. [PubMed: 16766026]
15. Lim F, Sun AM. Microencapsulated islets as bioartificial endocrine pancreas. Science. 1980; 210(4472):908–910. [PubMed: 6776628]
16. Tam SK, Bilodeau S, Dusseault J, et al. Biocompatibility and physicochemical characteristics of alginate-polycation microcapsules. Acta Biomater. 2011; 7(4):1683–1692. [PubMed: 21145438]

Author Manuscript Author Manuscript Author Manuscript Author Manuscript

17. Orive G, Tam SK, Pedraz JL, Halle JP. Biocompatibility of alginate-poly-L-lysine microcapsules for cell therapy. Biomaterials. 2006; 27(20):3691–3700. [PubMed: 16574222]
18. Bhujbal SV, de Haan B, Niclou SP, de Vos P. A novel multilayer immunoisolating encapsulation system overcoming protrusion of cells. Sci Rep. 2014; 4:6856. [PubMed: 25358640]
19. Matsumotoa S, Tan P, Baker J, Durbin K, Tomiyaa M, Azumaa K, Doia M, Elliott RB. Clinical Porcine Islet Xenotransplantation Under Comprehensive Regulation. Transpl Proc. 2014; 46:1992–1995.
20. Arifin DR, Manek S, Call E, et al. Microcapsules with intrinsic barium radiopacity for immunoprotection and X-ray/CT imaging of pancreatic islet cells. Biomaterials. 2012
21. Barnett BP, Arepally A, Karmarkar PV, et al. Magnetic resonance-guided, real-time targeted delivery and imaging of magnetocapsules immunoprotecting pancreatic islet cells. Nat Med. 2007; 13(8):986–991. [PubMed: 17660829]
22. Arifin DR, Long CM, Gilad AA, et al. Trimodal Gadolinium-Gold Microcapsules Containing Pancreatic Islet Cells Restore Normoglycemia in Diabetic Mice and Can Be Tracked by Using US, CT, and Positive-Contrast MR Imaging. Radiology. 2011; 260(3):790–798. [PubMed: 21734156]
23. Barnett BP, Arepally A, Stuber M, et al. Synthesis of magnetic resonance-, X-ray- and ultrasound-visible alginate microcapsules for immunoisolation and noninvasive imaging of cellular therapeutics. Nat Protoc. 2011; 6(8):1142–1151. [PubMed: 21799484]
24. Fu YL, Kedziorek DA, Ouwerkerk R, et al. Novel Perfluorinated Alginate Microcapsules for CT and MRI Monitoring of Mesenchymal Stem Cell Delivery and Engraftment Tracking. Journal of the American College of Cardiology. 2009; 53(10):A447–A447.
25. Kedziorek DA, Hofmann LV, Fu Y, et al. X-ray-visible microcapsules containing mesenchymal stem cells improve hind limb perfusion in a rabbit model of peripheral arterial disease. Stem Cells. 2012; 30(6):1286–1296. [PubMed: 22438076]
26. Weiss CR, Nour SG, Lewin JS. MR-guided biopsy: a review of current techniques and applications. J Magn Reson Imaging. 2008; 27(2):311–325. [PubMed: 18219685]
27. Dawson, HD. The Minipig in Biomedical Research. Boca Raton: CRC Press; 2011. A comparative assessment of the pig, mouse and human genomes.
28. Link TW, Woodrum D, Gilson WD, et al. MR-guided portal vein delivery and monitoring of magnetocapsules: assessment of physiologic effects on the liver. J Vasc Interv Radiol. 2011; 22(9): 1335–1340. [PubMed: 21816623]
29. Link TW, Arifin DR, Long CM, et al. Use of Magnetocapsules for In Vivo Visualization and Enhanced Survival of Xenogeneic HepG2 Cell Transplants. Cell Med. 2012; 4(2):77–84. [PubMed: 23293747]
30. Mills PH, Hitchens TK, Foley LM, et al. Automated detection and characterization of SPIO-labeled cells and capsules using magnetic field perturbations. Magn Reson Med. 2012; 67(1):278–289. [PubMed: 21656554]
31. Beck, N. Diagnostic Hematology. London: Springer-Verlag London; 2009.
32. Bennet W, Groth CG, Larsson R, et al. Isolated human islets trigger an instant blood mediated inflammatory reaction: implications for portal islet transplantation as a treatment for patients with type 1 diabetes. Ups J Med Sci. 2000; 105(2):125–133. [PubMed: 11095109]
33. Hawthorne WJ, Salvaris EJ, Phillips P, et al. Control of IBMIR in neonatal porcine islet xenotransplantation in baboons. Am J Transplant. 2014; 14(6):1300–1309. [PubMed: 24842781]
34. Inoue M, Maeno T, Miki D, et al. Survival of subretinal pancreatic islet cell allografts and apoptosis in infiltrating lymphocytes in rats. Ophthalmic Res. 2004; 36(1):31–37. [PubMed: 15007237]
35. Ar'Rajab A, Dawidson IJ, Harris RB, Sentementes JT. Immune privilege of the testis for islet xenotransplantation (rat to mouse). Cell Transplant. 1994; 3(6):493–498. [PubMed: 7881761]
36. Pileggi A, Molano RD, Ricordi C, et al. Reversal of diabetes by pancreatic islet transplantation into a subcutaneous, neovascularized device. Transplantation. 2006; 81(9):1318–1324. [PubMed: 16699461]
37. Perez-Basterrechea M, Briones RM, Alvarez-Viejo M, et al. Plasma-fibroblast gel as scaffold for islet transplantation. Tissue Eng Part A. 2009; 15(3):569–577. [PubMed: 18694292]

Author Manuscript Author Manuscript Author Manuscript Author Manuscript

38. Luan NM, Iwata H. Long-term allogeneic islet graft survival in prevascularized subcutaneous sites without immunosuppressive treatment. Am J Transplant. 2014; 14(7):1533–1542. [PubMed: 24909185]
39. Balamurugan AN, Gu Y, Tabata Y, et al. Bioartificial pancreas transplantation at prevascularized intermuscular space: effect of angiogenesis induction on islet survival. Pancreas. 2003; 26(3):279–285. [PubMed: 12657955]
40. Witkowski P, Sondermeijer H, Hardy MA, et al. Islet Grafting and Imaging in a Bioengineered Intramuscular Space. Transplantation. 2009; 88(9):1065–1074. [PubMed: 19898201]
41. Dufrane D, Goebbels RM, Gianello P. Alginate macroencapsulation of pig islets allows correction of streptozotocin-induced diabetes in primates up to 6 months without immunosuppression. Transplantation. 2010; 90(10):1054–1062. [PubMed: 20975626]
42. Sterkers A, Hubert T, Gmyr V, et al. Islet survival and function following intramuscular autotransplantation in the minipig. Am J Transplant. 2013; 13(4):891–898. [PubMed: 23496914]
43. Song MY, Bae UJ, Jang KY, Park BH. Transplantation of betacellulin-transduced islets improves glucose intolerance in diabetic mice. Exp Mol Med. 2014; 46:e98. [PubMed: 24875130]
44. Loganathan G, Graham ML, Radosevich DM, et al. Factors affecting transplant outcomes in diabetic nude mice receiving human, porcine, and nonhuman primate islets: analysis of 335 transplantations. Transplantation. 2013; 95(12):1439–1447. [PubMed: 23677052]
45. Sakata N, Tan A, Chan N, et al. Efficacy comparison between portal and subcapsular islet transplants in a murine diabetic model. Transplant Proc. 2009; 41(1):346–349. [PubMed: 19249553]
46. Dufrane D, D'hoore W, Goebbels RM, et al. Parameters favouring successful adult pig islet isolations for xenotransplantation in pig-to-primate models. Xenotransplantation. 2006; 13(3):204–214. [PubMed: 16756563]
47. Kumagai N, LaMattina JC, Kamano C, et al. Vascularized islet cell transplantation in miniature Swine: islet-kidney allografts correct the diabetic hyperglycemia induced by total pancreatectomy. Diabetes. 2002; 51(11):3220–3228. [PubMed: 12401713]
48. Kumagai N, O'Neil JJ, Barth RN, et al. Vascularized islet-cell transplantation in miniature swine. I. Preparation of vascularized islet kidneys. Transplantation. 2002; 74(9):1223–1230. [PubMed: 12451257]
49. Vallabhajosyula P, Hirakata A, Shimizu A, et al. Assessing the effect of immunosuppression on engraftment of pancreatic islets. Transplantation. 2013; 96(4):372–378. [PubMed: 23883972]
50. Hawthorne WJ, Simond DM, Stokes R, et al. Pre-clinical model of composite foetal pig pancreas fragment/renal xenotransplantation to treat renal failure and diabetes. Xenotransplantation. 2011; 18(6):390–399. [PubMed: 22168145]
51. Hawthorne WJ, Simond DM, Stokes R, et al. Subcapsular fetal pig pancreas fragment transplantation provides normal blood glucose control in a preclinical model of diabetes. Transplantation. 2011; 91(5):515–521. [PubMed: 21183867]
52. Dufrane D, Goebbels RM, Saliez A, et al. Six-month survival of microencapsulated pig islets and alginate biocompatibility in primates: Proof of concept. Transplantation. 2006; 81(9):1345–1353. [PubMed: 16699465]

Author Manuscript Author Manuscript Author Manuscript Author Manuscript

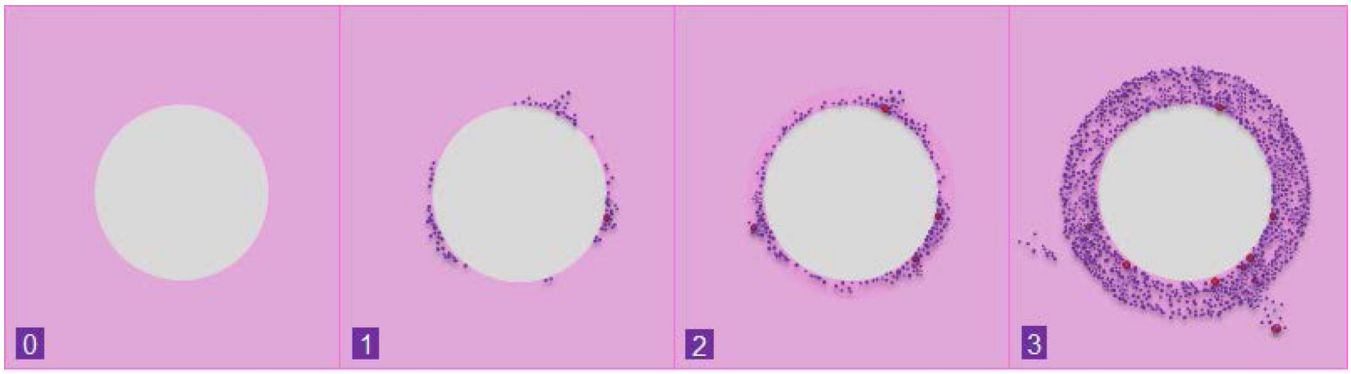

Figure 1.

Schematic diagrams illustrating the histopathological scoring scale for the occurrence of IIR and FBR. 0= Essential no immune or fibrotic response; 1= Partial immune or fibrotic response that does not encompass the entire circumference of a capsule; 2 = Complete circumferential immune response; 3 = A thick cap of fibrosis with intense inflammation. Purple dots=immune cells, red dots=eosinophils.

Author Manuscript Author Manuscript Author Manuscript Author Manuscript

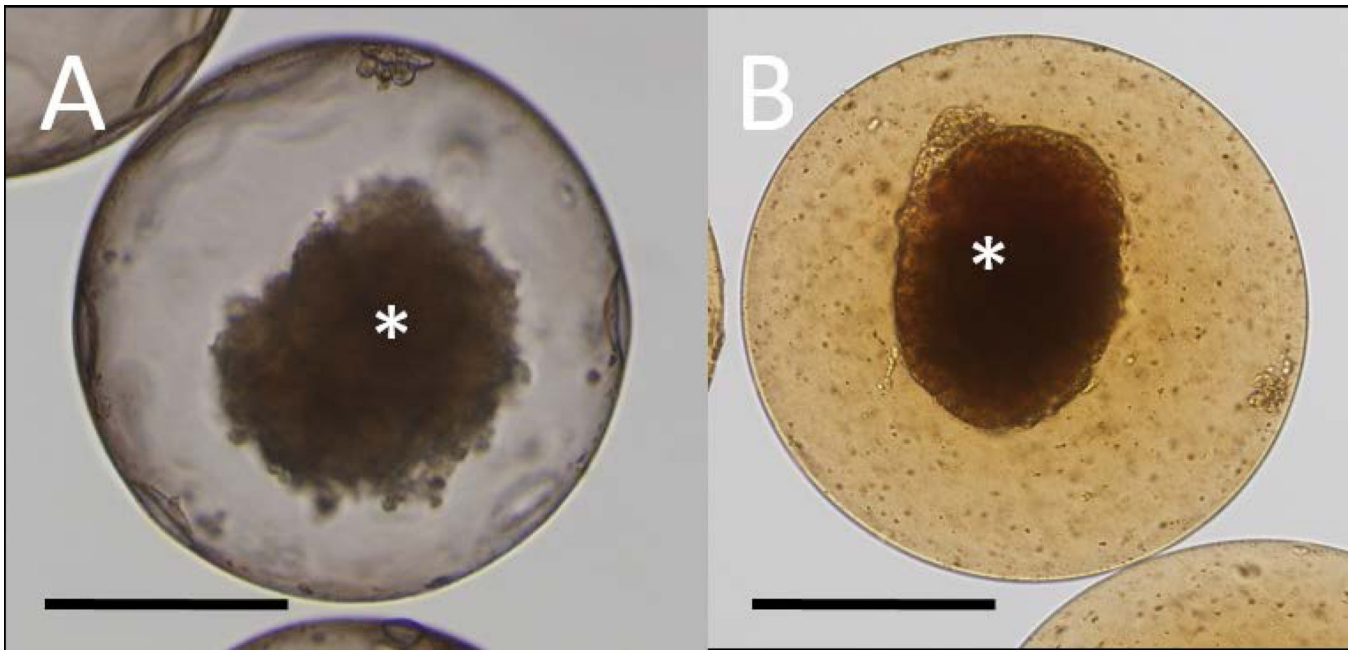

Figure 2.

Microscopic images of human islets in an APSA microcapsule without Feridex® (A) and with Feridex® (B). Feridex® causes brown colorization of magnetocapsules. Asterisks indicate human islets inside the microcapsule. Scale bar=200 μm.

Author Manuscript Author Manuscript Author Manuscript Author Manuscript

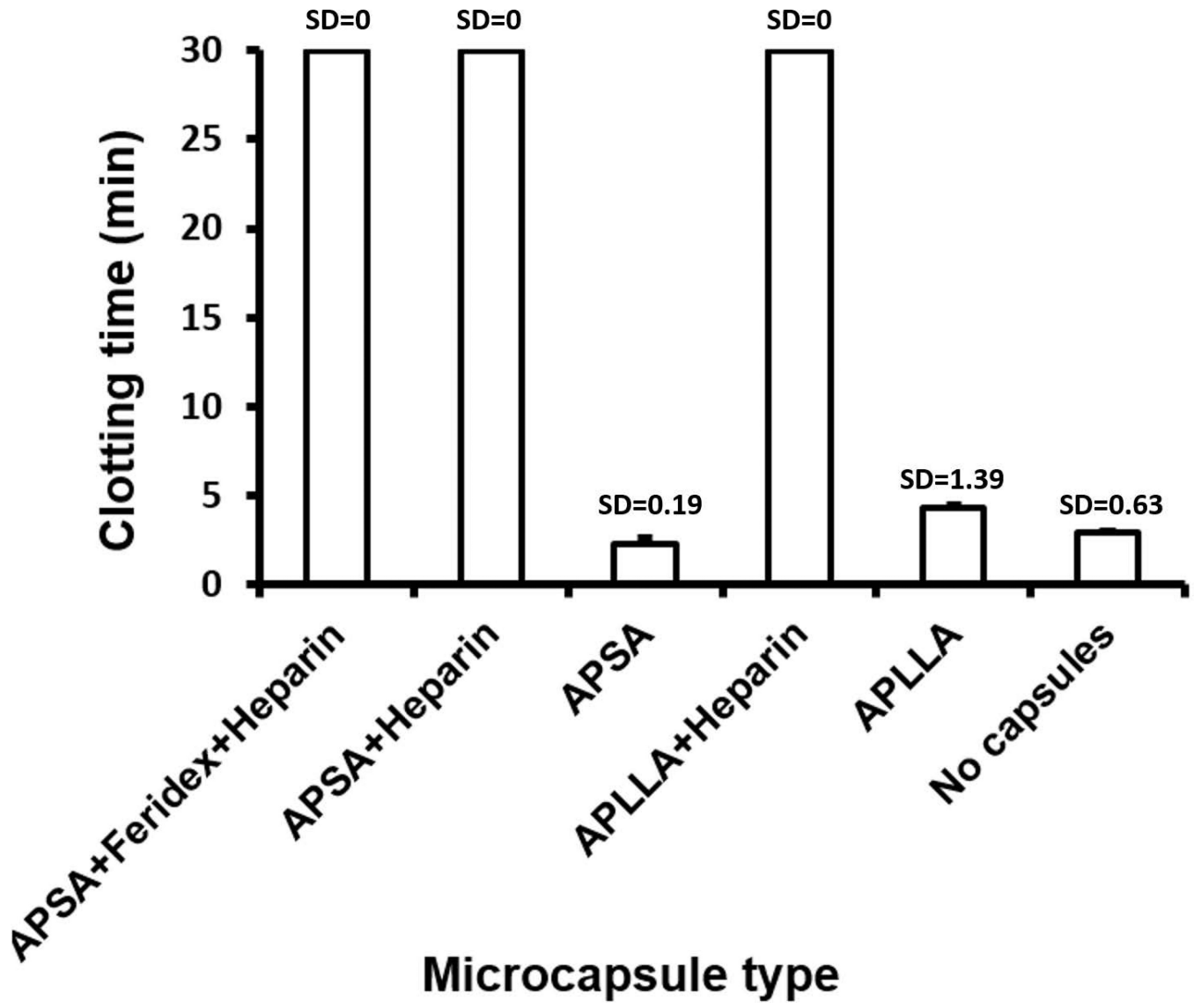

Figure 3.

In vitro blood clotting times for the different microcapsule formulations as determined using a Lee-White blood coagulation test. APSA+Feridex+Heparin, APSA+Heparin and APLLA +Heparin capsules did not cause blood coagulation for >48 hours. SD = standard deviations.

Author Manuscript Author Manuscript Author Manuscript Author Manuscript

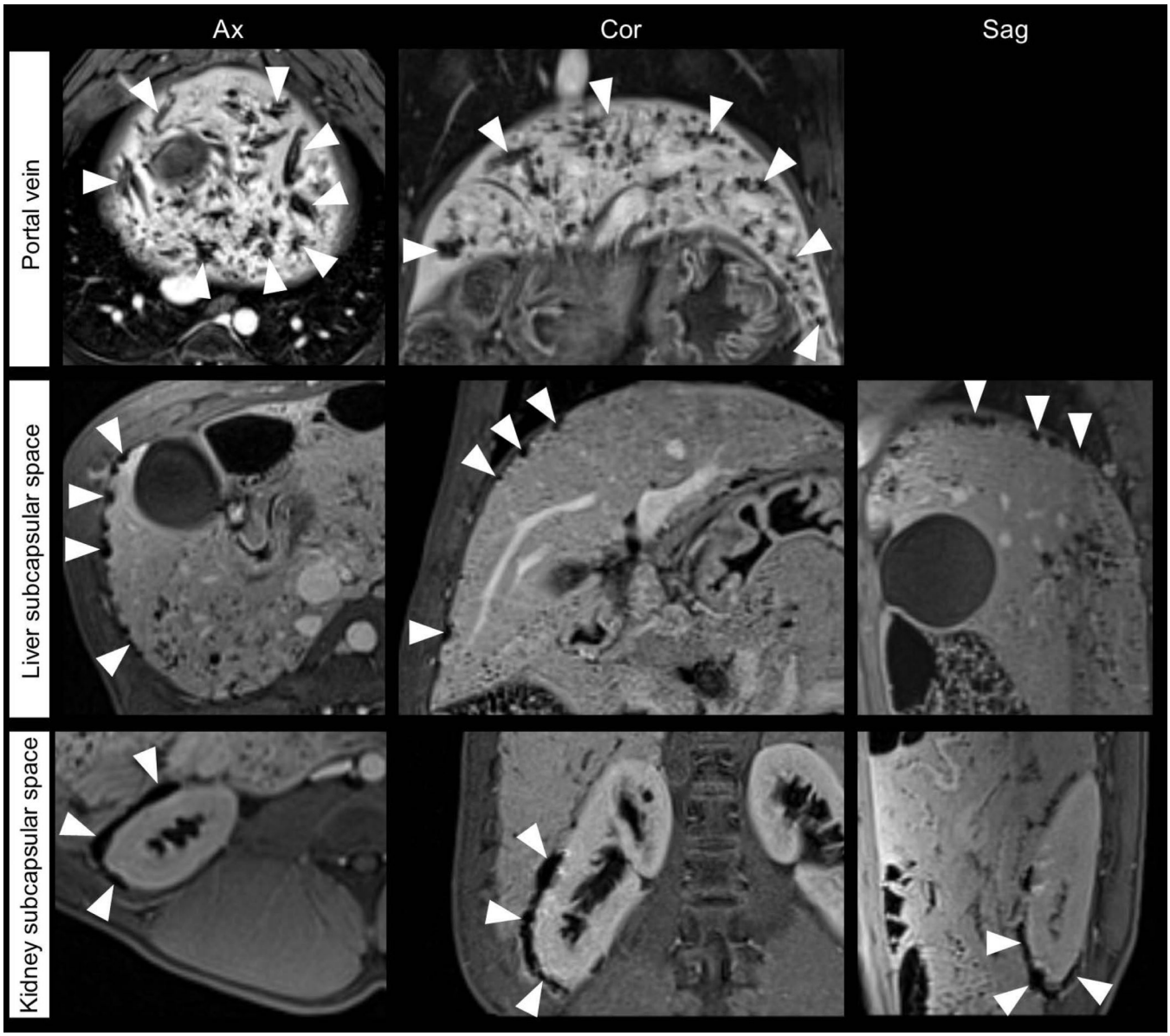

Figure 4.

Representative 1.5T MR images of magnetocapsules transplanted in the liver portal vein, liver subcapsular space and kidney subcapsular space. Arrowheads point to magnetocapsules as hypointense signals in the transplantation sites, providing a visual evidence of accurate injection. Ax = axial, Cor = coronal, Sag = sagittal.

Author Manuscript Author Manuscript Author Manuscript Author Manuscript

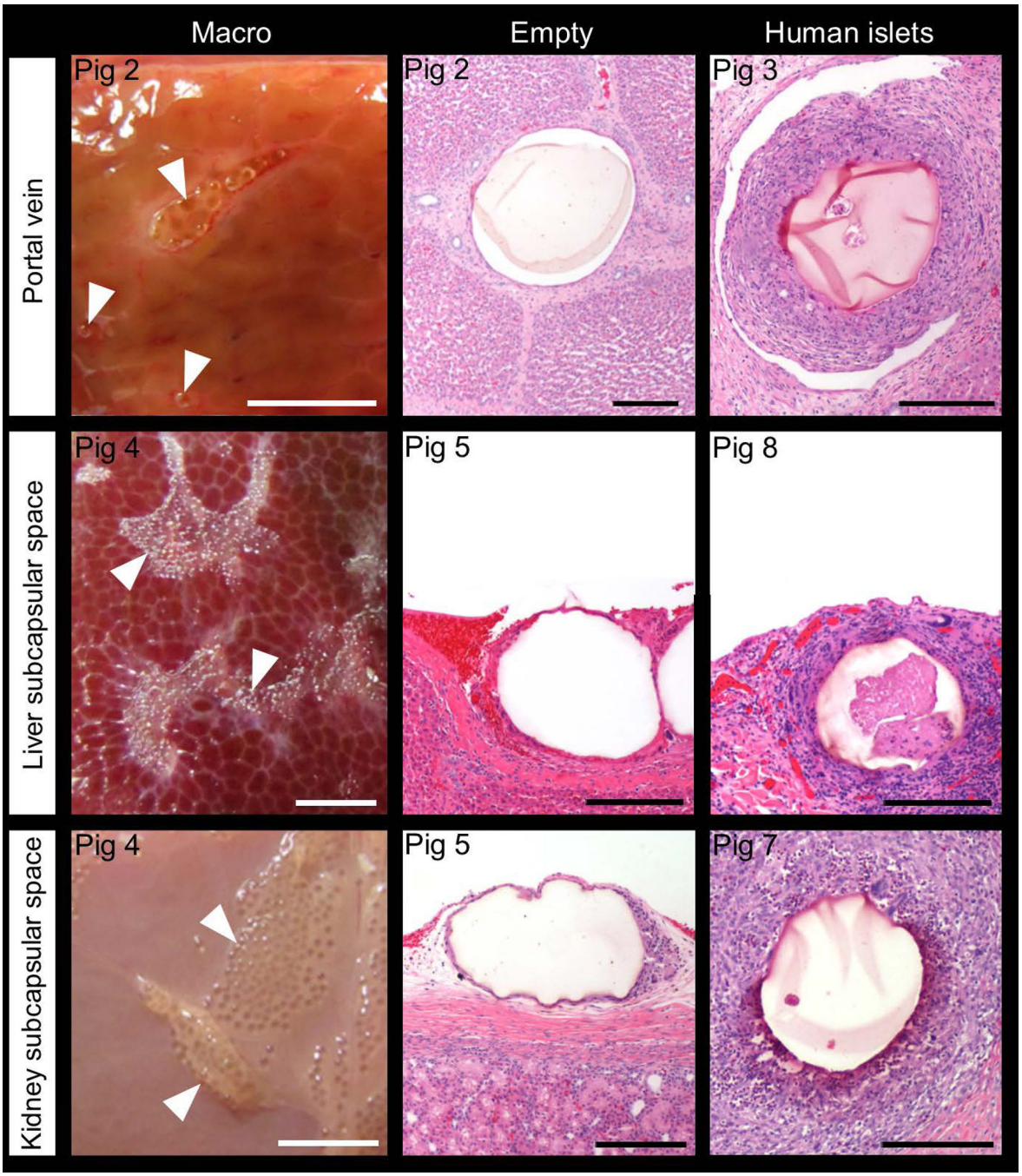

Figure 5.

Representative macrophotographs and H&E stained microscopic images of magnetocapsules transplanted in the liver portal vein, liver subcapsular space or kidney subcapsular space without (“empty”) or with human islets. Swine were allowed to survive for 2 weeks. Arrowheads indicate magnetocapsules. White scale bar = 5 mm, black scale bar = 200 μm.

Author Manuscript Author Manuscript Author Manuscript Author Manuscript

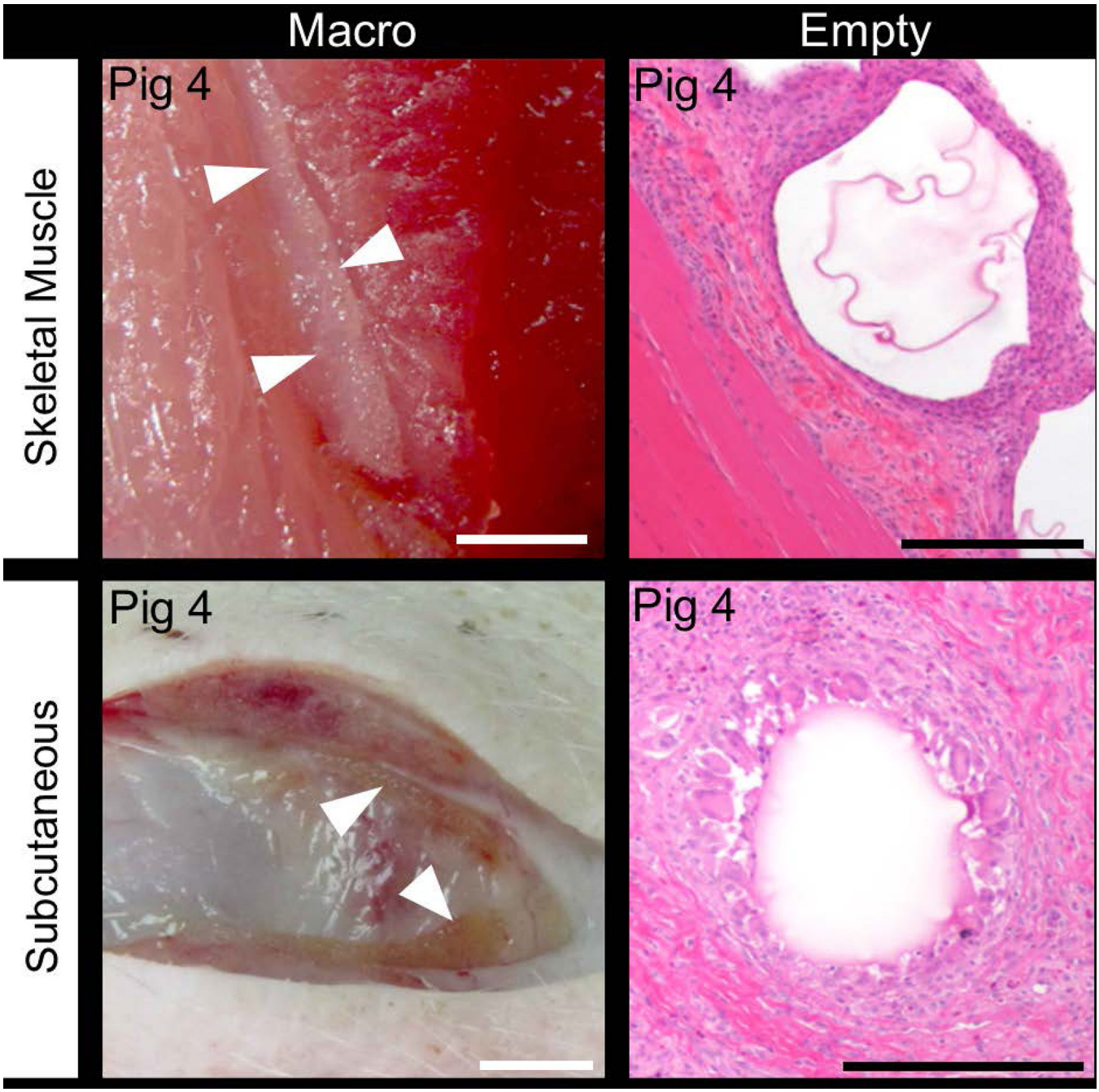

Figure 6.

Representative macrophotographs and H&E stained images of magnetocapsules transplanted in the skeletal muscle and subcutaneous sites. Swine were allowed to survive for 2 weeks. Arrowheads indicate microcapsules. White scale bar = 5 mm, black scale bar = 200 μm.

Author Manuscript Author Manuscript Author Manuscript Author Manuscript

Table 1

Summary of transplantation variables and histology outcome.

Pig ID	Human islets	TX	Surv (week)	OHS	IIR	FBR	IS	SS	TIR (μm)
1	−	PV	0	0	0.2	0	0.4	0.6	0.00±0.00
2	−	PV	2	2	0.6	1.6	0	1	22.00±17.15
3	+	PV	2	2.2	0.8	1.4	0.4	0.6	142.90±59.27
4	−	SC	2	3	1.7	0.4	1	0	51.30±20.12
4	−	SM	2	2.3	0.4	0.2	1	0	56.49±25.28
4	−	LS	2	1.8	0	0	0	1	21.17±11.26
4	−	KS	2	2	0	0	0	0.8	15.83±10.72
5	−	LS	2	1.3	0.3	0	0	1	20.83±7.35
5	−	KS	2	2	1	0.5	0.5	0.5	26.36±18.91
6	−	LS	2	1.3	0.3	0	0	1	18.92±12.70
6	−	KS	2	2	1	0.3	0.7	0.3	17.22±10.82
7	+	KS	2	2	1	1	1	0	192.47±63.26
8	+	LS	2	2	0.8	0.6	1	0	78.50±37.02
8	+	KS	2	2.4	1.4	0.4	1	0	151.11±64.20

TX=transplantation site, PV=portal vein, SC=subcutaneous, SM=skeletal muscle, LS=liver subcapsular space, KS=kidney subcapsular space, Surv=survival period in weeks, OHS=overall histology score, IIR = Innate immune response, FBR=foreign body reaction, IS=inflammation score, SS=stromal score, TIR=Thickness of immune response

Xenotransplantation. Author manuscript; available in PMC 2017 May 26.

Author Manuscript

Author Manuscript

Author Manuscript

Author Manuscript

Table 2

Formulations of the different alginate microcapsules that were screened using a Lee-White blood coagulation test.

Microcapsule type	Polycation	Surface treatment
APSA	Protamine sulfate	None
APSA+Heparin	Protamine sulfate	Heparin coating
APLLA	Poly-L-lysine	None
APLLA+Heparin	Poly-L-lysine	Heparin coating